Original Article

PROGRESS in MEDICAL PHYSICS Vol. 27, No. 2, June, 2016
http://dx.doi.org/10.14316/pmp.2016.27.2.55

Modulation Transfer Function with Aluminum Sheets of Varying Thickness

Dong Joo Rhee*, Me Young Kim*, Young Min Moon†, Dong Hyeok Jeong*

*Research Center, †Department of Radiation Oncology,
Dongnam Institute of Radiological and Medical Sciences, Busan, Korea

We studied the method to gain a clear LSF using a thick aluminum sheet and to acquire the spatial resolution value with a high accuracy for a low spatial resolution imaging modality. In this study, aluminum sheets with thicknesses varying from 0.3 mm to 1.2 mm were tested to derive a modulation transfer function (MTF) for the oversampling and non-oversampling methods. The results were evaluated to verify the feasibility of the use of thick sheets for periodic quality assurance. Oversampling was more accurate than non-oversampling, and an aluminum sheet with a correction factor less than 2 at the cut-off frequency, which was less than 0.8 mm in this case, was confirmed to be suitable for MTF measurements. Therefore, MTF derivation from a thick aluminum sheet with thickness correction is plausible for a medical imaging modality.

Key Words: Modulation transfer functions, Image spatial resolution, Oversampling method

Introduction

The spatial resolution of computed tomography (CT) can be quantified by modulation transfer function (MTF), and various methods of its implementation using small beads, edge detection, and oversampling have been developed.[1-10] With these methods, the line spread function (LSF) of a CT scanner is acquired, and an MTF is derived by applying a Fourier transform to the acquired LSF. An oversampling LSF acquisition method using thin aluminum sheets, suggested by Boone,[1] gained popularity because of its high accuracy, and is thus used as a reference method for testing new LSF techniques.[11] However, studies on sheet thickness for LSF acquisition in varying conditions were insufficient. When Boone originally suggested LSF acquisition using the oversampling method with aluminum sheets, thin (0.05 mm) aluminum foils were commonly used to avoid thickness effects in the resulting LSF images. However, thin sheets might not be clearly imaged for some CT scanners or newer imaging modalities such as CBCT, because of their relatively poor image quality and large pixel size. Furthermore, determination of the slant angle of tilted samples is subjective, depending on the user, so reproducing the same phantom angulations can be challenging. Therefore, oversampling-based MTF measurement for periodic CT and CBCT quality assurance (QA) programs remains inconvenient and limited.

However, thick sheets can achieve clearer and less noisy LSFs than that of the less thick sheets, and were tested in this study for MTF calculation with a thickness correction in frequency space. Furthermore, a method of acquiring LSFs from parallel non-oversampling as opposed to tilted oversampling was tested for its feasibility as a QA method because of its convenience and a reduction in the uncertainties caused by angulations although the number of data points was limited. In this study, LSFs and corresponding MTFs were derived for aluminum sheets of varying thickness, both for oversampling and non-oversampling methods, and the results were compared to evaluate their accuracy and determine an optimized sheet thickness. Additionally, effects on the resultant MTF from the subjective choice of the angulation were evaluated. Finally, the

This research was supported by National R&D program through the Dongnam Inst. of Radiological & Medical Sciences, funded by the Ministry of Science, ICT and Future Planning (50495-2016).
Received 2 June 2016, Revised 9 June 2016, Accepted 10 June 2016
Correspondence: Dong Hyeok Jeong (physics7@empas.com)
Tel: 82-51-720-5813, Fax: 82-51-720-5826

thicknesses of the slabs holding the sheets as a background material were varied to estimate the effects of beam hardening on MTF calculations.

Materials and Methods

1. LSF acquisition

LSFs were acquired from images of the aluminum sheets sandwiched by solid water phantoms (Gammex, Middleton, WI), as shown in Fig. 1. Each slab has a density of 1.04 g/cm^3 and a size of 30 cm×30 cm×5 cm. A GE LightSpeed CT scanner (GE Healthcare, Waukesha, WI) was used to obtain images with a 120 kVp tube voltage, 330 mA beam current, and a 2.5 mm slice thickness. All of the images were reconstructed with the scanner's standard kernel option. The pixel size of each image was 0.29×0.29 mm^2, thus the Nyquist frequency of the image was determined to be 17.2 cm^{-1}, which exceeded the estimated cutoff frequency of the scanner (8.0 cm^{-1}) under the given condition.

For LSF acquisition, 200 vertical projections in the ROIs marked in Fig. 1. were averaged (parallel) or merged (tilted) for each CT slice of the image, after setting the background to zero by subtraction. The angle of the slope for each tilted image was determined with the image analysis software ImageJ (National Institute of Health, Bethesda, MD). To acquire a sufficient number of data points for Fourier transformation, LSFs from the non-oversampling method were interpolated to have the same number of data points as the oversampling method. In total, 50 LSFs were obtained for both methods, from 50 CT slices at each sheet thickness.

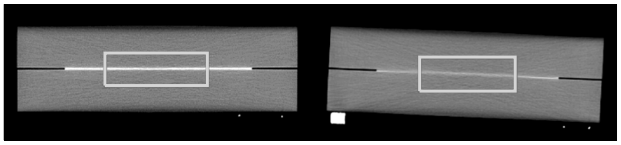

Fig. 1. Aluminum sheet images in the transverse plane for parallel non-oversampling LSF (left) and tilted oversampling LSF (right). The LSF was determined by the sum of all the vertical projections across the plane within the regions of interest (red boxes). Phase correction was applied for the oversampled LSF.

2. Thickness corrections

Aluminum sheets of seven different thicknesses were tested, from 0.3 mm to 1.2 mm. Their shapes were modeled as a rectangular function $\prod(\frac{x}{\mathrm{L}})$ in 2D, with thickness L. These varying thicknesses were compensated by applying a thickness correction in spatial-frequency space, according to Villafana's method for 2D X-ray-image MTF measurement.[12] $\mathrm{MTF_a}$, the acquired MTF before applying the sheet thickness correction, is derived from the acquired LSF ($\mathrm{LSF_a}$),

$$\mathrm{MTF_a}(v) = \mathrm{FT}\{\mathrm{LSF_a}(x)\} \tag{1}$$

where the variable v represents the spatial-frequency space corresponding to the object space, x. The true LSF of the imaging system, $\mathrm{LSF_T}$, is defined as the image of an infinitesimally narrow object. $\mathrm{LSF_T}$ was convolved with a rectangular function to represent the image acquired from the CT scanner, $\mathrm{LSF_a}$, so the relationship between $\mathrm{LSF_T}$ and $\mathrm{LSF_a}$ is

$$\mathrm{LSF_a}(x) = \mathrm{LSF_T}(x) * \prod(\frac{x}{\mathrm{L}}) \tag{2}$$

where the * symbol represents convolution. By applying the Fourier transform to both sides of equation (2), the left hand side becomes equivalent to equation (1), while the right hand side becomes

$$\mathrm{FT}\{\mathrm{LSF_T}(x) * \prod(\frac{x}{\mathrm{L}})\} = \mathrm{MTF_T}(v) \times \mathrm{L} \cdot \mathrm{sinc}(v\mathrm{L}) \tag{3}$$

where MTFT represents the true MTF of the overall imaging system: the Fourier transform of $\mathrm{LSF_T}$. Therefore, the $\mathrm{MTF_T}$, derived from the equation (1), (2), and (3), is

$$\mathrm{MTF_a}(v) = \mathrm{MTF_T}(v) \times \mathrm{L} \cdot \mathrm{sinc}(v\mathrm{L}) \tag{4}$$

$$\mathrm{MTF_T}(v) = \frac{1}{\mathrm{L} \cdot \mathrm{sinc}(v\mathrm{L})} \times \mathrm{MTF_a}(v) \tag{5}$$

where the correction factor is defined as the term multiplied by $\mathrm{MTF_a}$ in equation (5), and represents the discrepancy between $\mathrm{MTF_T}$ and $\mathrm{MTF_a}$ (reported for varied thickness in Fig. 2). From equation (5), the correction factor becomes infinitely high when the thickness of the sheet L reaches 1/v. Thus, with

a cutoff frequency of 8.0 cm^{-1}, 1.25 mm is the thickest sheet used for the MTF measurements. For the 0.3 mm sheet, the correction factor reaches a limit of 1.1 at the estimated cutoff frequency of the system, 8.0 cm^{-1}; for the 1.2 mm sheet, the correction factor becomes 24.

3. LSF verification

In order to validate the accuracy of the measured LSF, a point spread function (PSF) verification method suggested by Ohkubo et al.[13] was adopted. A 2D PSF in the scan plane was derived from the 1D LSF, on the assumption that the PSF has rotational symmetry in this plane.[14] The 2D PSF, PSF(x,y), was convolved with the object, Obj(x,y), of known size and material. By definition, this result became the estimated CT image of the object, Img(x,y), as follows:

$$\mathrm{Img}(x,y) = \mathrm{PSF}(x,y) ** \mathrm{Obj}(x,y) \tag{6}$$

where ** represents a 2D convolution. In theory, since the derived PSF closely matched the shape of the real PSF of the system, Img(x,y) resembled the real CT image, CTImg(x,y), of Obj(x,y) if the noise level of the system was acceptably low and consistent. Therefore, the similarity between Img(x,y) and CTImg(x,y) represents the accuracy of the derived 2D PSF, and the accuracy of the LSF may be evaluated accordingly. In this study, the accuracy of the 2D PSF was quantified by the standard deviation (SD) of the discrepancy between the estimated and real CT images, which was defined as

$$\mathrm{SD} = \sqrt{\frac{\sum_{i,j}(\mathrm{Img}(i,j) - \mathrm{CTImg}(i,j))^2}{\max(i) \times \max(j)}} \tag{7}$$

where i and j represent the pixel indices in the x and y directions, respectively, and thus max(i)×max(j) represent the total number of pixels in the images.

A Teflon cylinder in the Catphan 504 phantom (Phantom Laboratory, Salem, NY) was chosen as the object for this study due to its low noise level and consistency when imaged

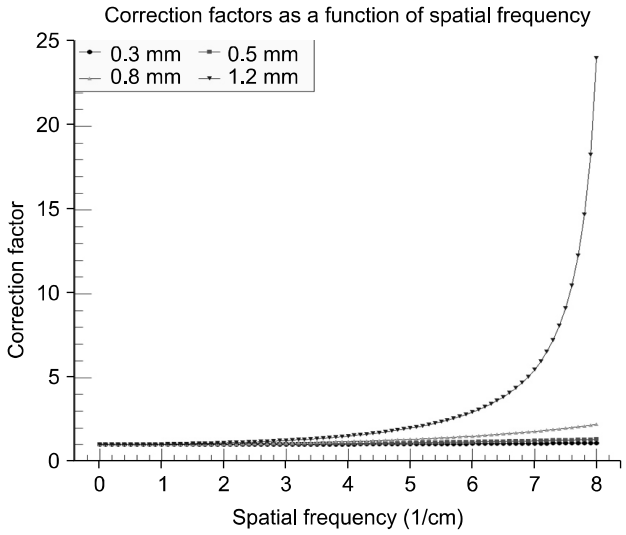

Fig. 2. Correction factors as a function of spatial frequency with different slab thicknesses. As the sheet becomes thicker and the spatial frequency becomes higher, the correction factor increases.

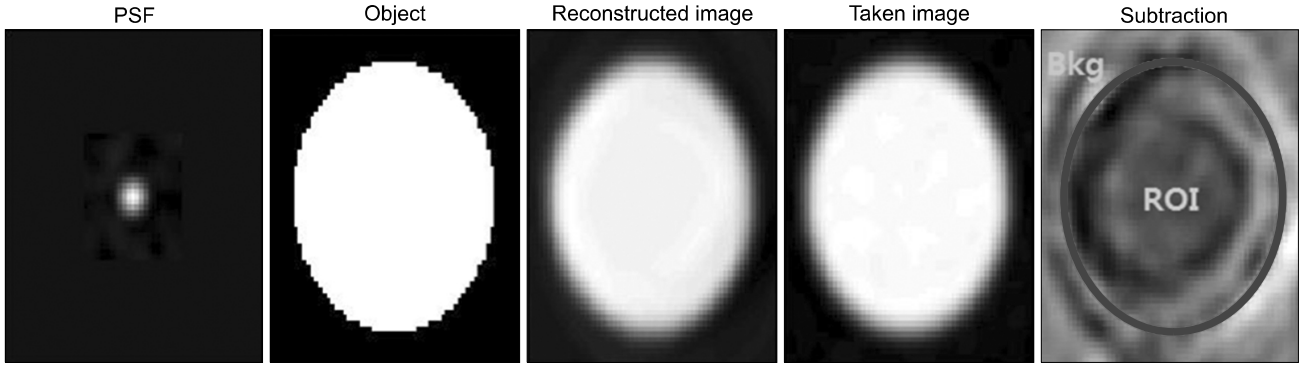

Fig. 3. 2D PSF reconstructed from LSF was convolved with the object to compute the constructed image. The constructed image was compared with the real CT image of the object by subtraction. The region of interest (ROI) was determined as the size of the object, with background as the remained of the image. The standard deviation of the subtracted images were evaluated both separately and in combination.

by CT. The diameter of the object was 12.3 mm and the CT number with the designated kVp was 980 Hounsfield Units (HU) for Teflon and 30 HU for the surrounding material. The subtracted image was separated into ROI and background (BKG) as shown in Fig. 3; the standard deviation of the ROI, BKG, and full image were calculated separately.

To quantify the SD for comparison, a normalized SD (NSD) was computed[13,15] as follows:

$$\mathrm{NSD} = \frac{\mathrm{SD}}{(\mathrm{CT1} - \mathrm{CT2})} \times 100\% \tag{8}$$

where CT1 and CT2 are the constant CT numbers for the Teflon cylinder and the surrounding object (980 HU and 30 HU, respectively).

4. MTF comparison

Although the PSF verification method evaluates the accuracy of the measured LSF, it does not indicate whether LSF and MTF were over- or underestimated. Therefore, comparison of MTFs at different spatial frequencies is required to evaluate outcomes. MTF is defined as the magnitude of the Fourier Transform of the LSF and in this study, fast Fourier transform (FFT) was used for deriving the MTF from LSF. The MTF was normalized to a spatial frequency of zero. MTF 50, MTF 10, and MTF 5, the spatial frequencies at which MTF becomes 0.5, 0.1, and 0.05, respectively, were measured and compared for each data set. The units for MTF are cm^{-1} throughout this paper.

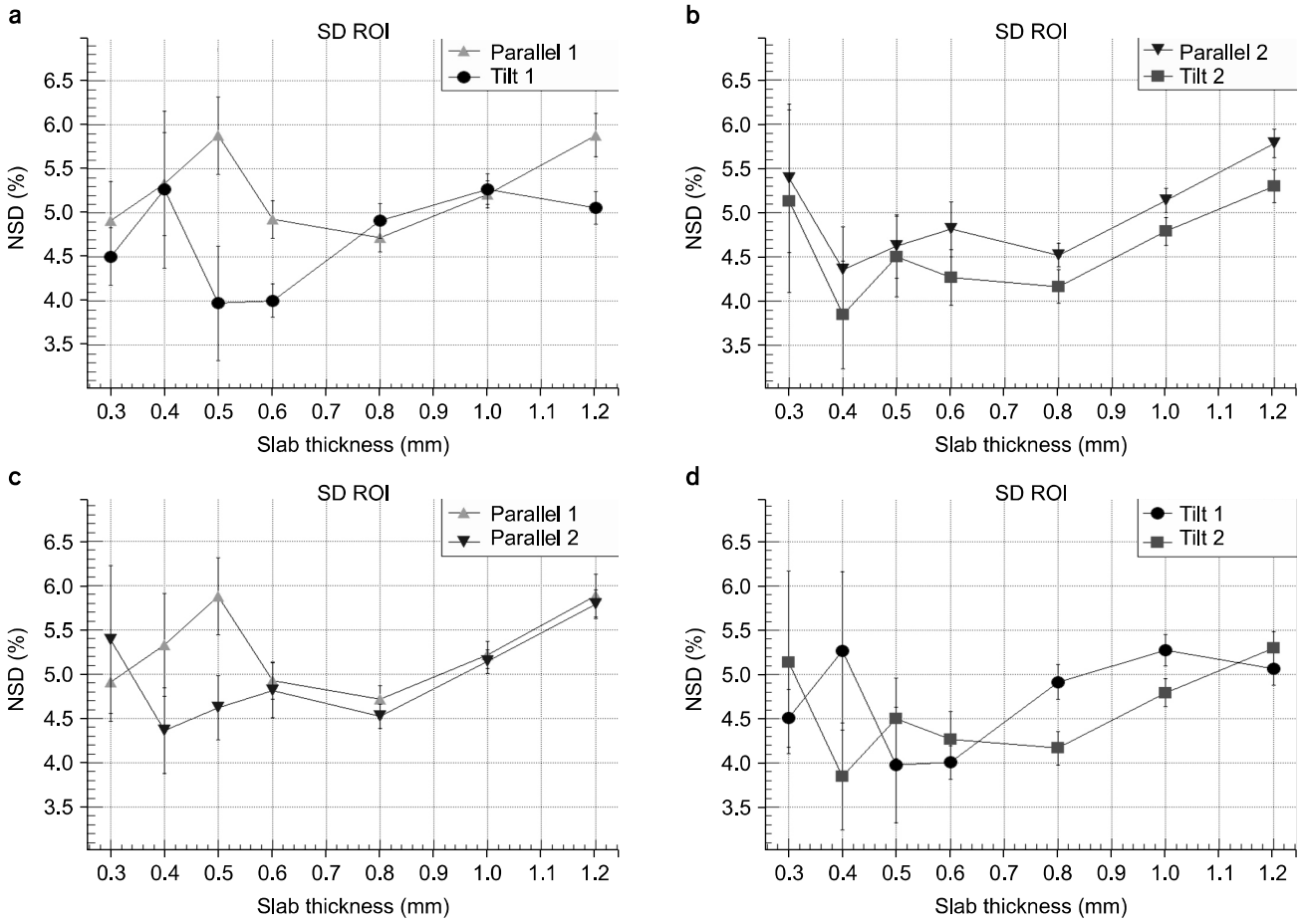

Fig. 4. Normalized standard deviation of the region of interest (ROI) in the subtracted image. Parallel 1 (triangle) and Tilt 1 (circle) are compared in (a), Parallel 2 (inverted triangle) and Tilt 2 (square) are compared in (b), Parallel 1 and 2 are compared in (c), and Tilt 1 and 2 are compared in (d).

5. Beam-hardening effect

The low energy X-rays in a polychromatic beam from the CT scanner have shorter path lengths than those of high energy X-rays, so the average energy of the spectrum increases as the beam passes through a material; this phenomenon is called beam hardening.[16,17] Therefore, the thickness of the background material can alter the degree of the beam-hardening effect, as well as the final image, which may affect the shape of an acquired LSF and MTF. All measurements were performed with one and two solid-water slab pairs sandwiching the aluminum sheet, to see whether the beam-hardening effect by the background material significantly changed the LSF and the MTF.

6. Angle variations in oversampling method

The angle of the slope for the oversampling method was determined manually, so the choice of angle was inevitably subjective. The results from the oversampling method must be reproduced by different operators to be considered reliable for quality assurance. To quantify the deviations from the different selection of the angles, MTF 50, 10, and 5 were measured for six different angles from 2.0^{o} to 3.0^{o} in increments of 0.2^{o}. Sheet thicknesses of 0.4 mm and 0.6 mm with one pair of water slabs were used, as these conditions gave the most unreliable and reliable results, respectively, as shown later.

Results

Standard deviations of the subtracted images with various

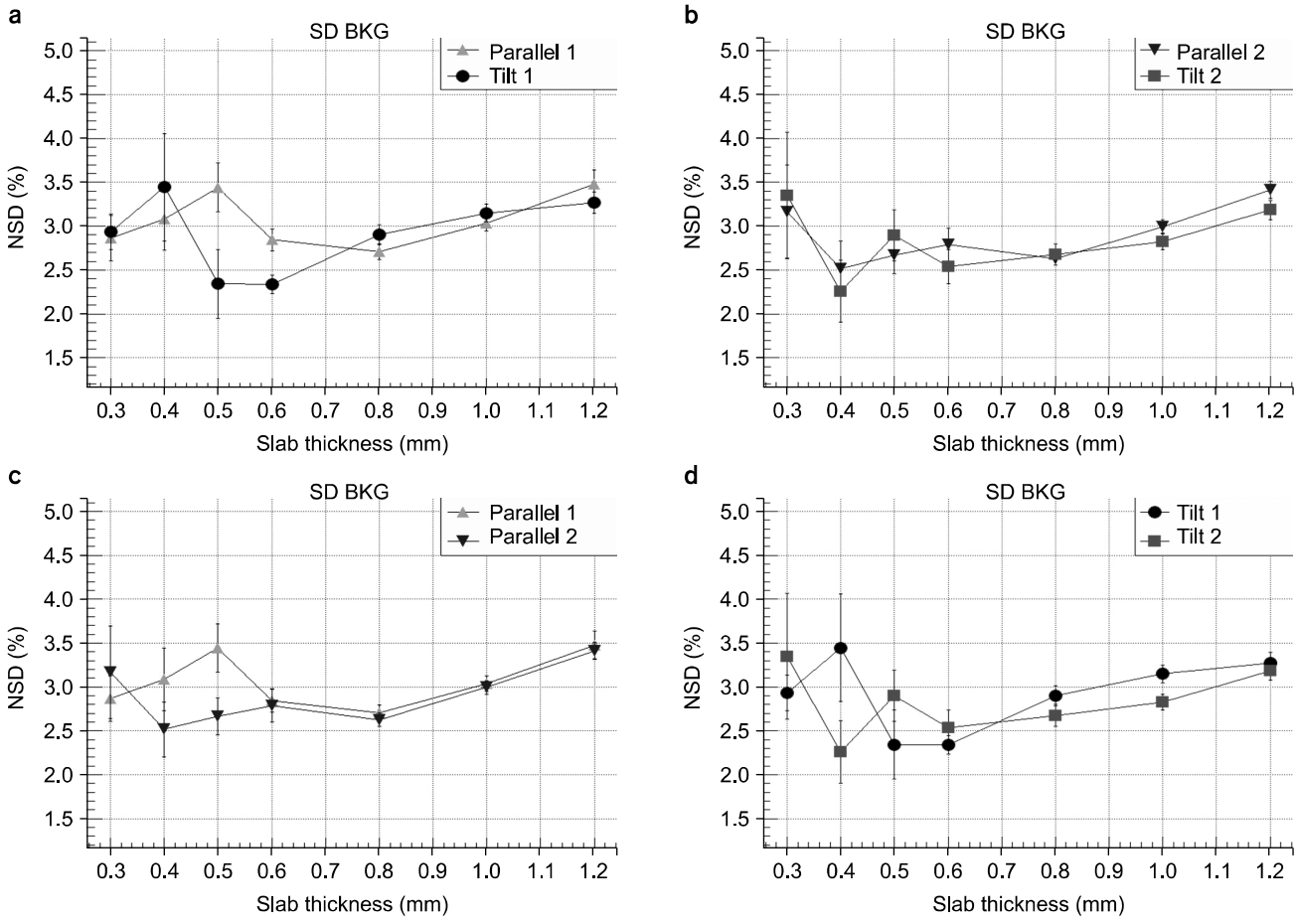

Fig. 5. Normalized standard deviation of the background (BKG) region in the subtracted image.

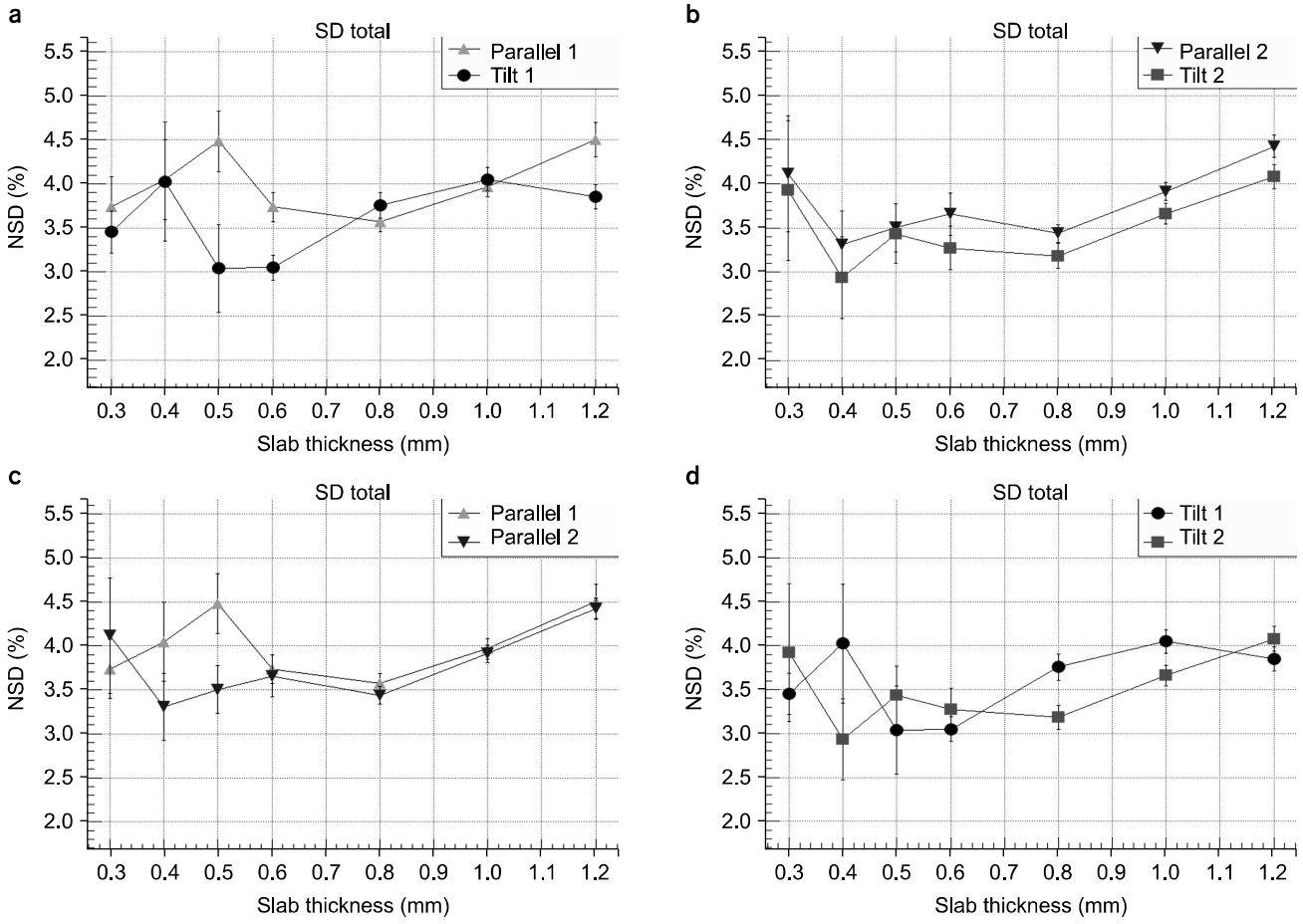

Fig. 6. Normalized standard deviation of the subtracted image including both ROI and BKG.

sheet thicknesses are presented in Fig. 4, 5, and 6; these represent the normalized standard deviations (NSD) for the region of interest, the background, and the total subtracted image, respectively. The following methods are compared in each figure: oversampling with one pair of slab background (Tilt 1), oversampling with two pairs of slab background (Tilt 2), non-oversampling with one pair of slab background (Parallel 1), and non-oversampling with two pairs of slab background (Parallel 2). By definition, the measured LSF approaches the systems true LSF as NSD is minimized. Each point in the plot indicates the arithmetic mean of the NSD from 50 LSFs and the error bar indicates one standard deviation (1σ) of the 50 NSDs.

MTF 50, 10, and 5 as a function of the sheet thickness are presented in Fig. 7(a), (b), (c) respectively. Parallel 1 and Tilt 1, Parallel 2 and Tilt 2, Parallel 1, 2 and Tilt 1, 2 were compared for each set of MTFs. The error bars also indicate one standard deviation (1σ) of the dataset.

1. Sheet thickness

Overall, the variations in NSD were significantly large for sheets thinner than 0.5 mm (Fig. 4, 5, and 6). NSD tended to increase for sheets thickness beyond 1 mm. In general, SD BKG (Fig. 5) was less dependent on sheet thickness than SD ROI (Fig. 4).

MTF 50 was not dependent on the sheet thickness for oversampling or non-oversampling, as shown in Fig. 7(a). MTF 10 and MTF 5 show a correlation up to 0.8 mm but significantly changed beyond 1.0～1.2 mm thickness.

2. Oversampling and non-oversampling methods

The oversampling method gave more accurate results in Fig.

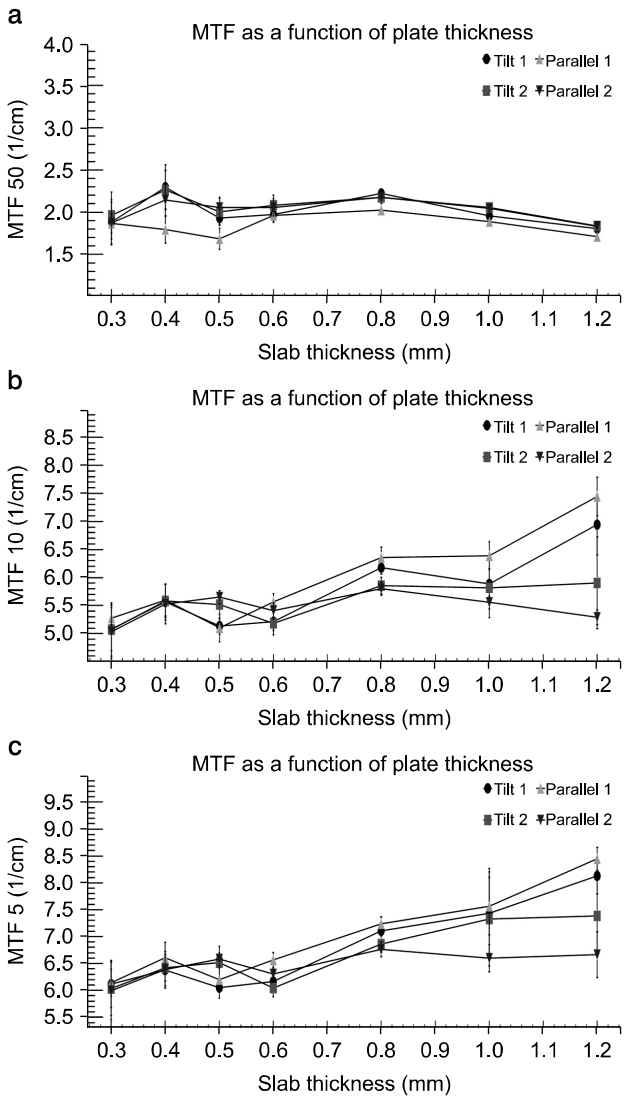

Fig. 7. MTFs as a function of sheet thickness. MTF 50 (a), MTF 10 (b), and MTF 5 (c) for Tilt 1, Tilt 2, Parallel 1, and Parallel 2 cases are presented.

4(b) and 6(b), with negligible improvement for the background region, (Fig. 5(b)). When one slab was used, the oversampling method was more accurate than the non-oversampling method for 0.5, 0.6, and 1.2 mm, with insignificant differences for the rest of the sheets in Fig. 4(a) and 6(a).

No significant differences between oversampling and non-oversampling methods for MTF 50 were observed. For MTF 10 and MTF 5, however, the difference between the oversampling methods (Tilt 1 and Tilt 2) was much smaller than that of the non-oversampling method (Parallel 1 and Parallel 2) when the 1.0 and 1.2 mm thickness sheets were used.

Table 1. Variations in MTFs according to the determination of the slope angle in the oversampling method.[a]

Angle (°)	MTF 50	MTF 10	MTF 5
2.0	1.972±0.090	5.219±0.158	6.183±0.155
2.2	1.980±0.095	5.245±0.158	6.228±0.159
2.4	1.981±0.093	5.255±0.158	6.244±0.170
2.6	1.981±0.094	5.254±0.160	6.235±0.184
2.8	1.976±0.092	5.237±0.160	6.221±0.176
3.0	1.968±0.091	5.214±0.153	6.200±0.169
Max diff.	0.013	0.041	0.061

[a]0.6 mm aluminum sheet with one water-slab pair used to acquire the data with maximum 1° variations.

Table 2. Variations in MTF according to the determination of the slope angle in the oversampling method.[a]

Angle (°)	MTF 50	MTF 10	MTF 5
2.0	2.264±0.261	5.531±0.305	6.349±0.270
2.2	2.283±0.265	5.560±0.305	6.362±0.282
2.4	2.290±0.269	5.562±0.319	6.378±0.294
2.6	2.291±0.270	5.560±0.323	6.371±0.301
2.8	2.280±0.270	5.520±0.340	6.332±0.319
3.0	2.267±0.270	5.479±0.337	6.326±0.339
Max diff.	0.027	0.031	0.052

[a]0.4 mm aluminum sheet with one water-slab pair used to acquire the data with maximum 1° variations.

3. Number of slabs

No significant differences between one pair and two pairs of background material slabs were shown in Fig. 6(c) and 6(d), except for the 0.5 mm sheet with non-oversampling, and the 0.8 and 1.0 mm sheets with oversampling. The difference is less significant in the background region, as shown in 5(c) and 5(d).

For the oversampling method, the number of slabs did not affect MTF 50, 10, and 5 significantly. On the other hand, Parallel 1 and Parallel 2 show the significant differences in MTF 10 and MTF 5 for sheets thicker than 1.0 mm.

4. Effect of the angle variations

MTF variations, by the subjective choice of angles for 0.6 mm and 0.4 mm sheets, are shown in Table 1 and 2, respectively. The confidence interval in the tables is 1σ of the

measured MTFs. The maximum differences are between the largest and the smallest MTFs among the six angles. For all the reported MTFs, differences due to angular variation were much smaller than the inherent MTF variations from the data.

Discussion

The thin-aluminum-sheet oversampling method is advantageous over other methods in terms of the number of the data points producing the LSF. However, newer imaging modalities such as CBCT have relatively poor image resolution and large pixel size, so thicker sheets are required. The accuracy of the LSFs acquired from various thicknesses of aluminum sheets were quantified by NSD, and the values ranged from 3.0 to 4.5% (Fig. 6). These results are compatible with the conventional thin-sheet oversampling method, since the LSF measurements with a 0.05 mm aluminum sheet gave an NSD of 2.2 to 4.5%, depending on the choice of reconstruction kernels by Ohkubo et al.[13] in similar measurement conditions. Most discrepancies between the measured image and the reconstructed image were from the ROI, especially at the edge of the object, since the NSD of the ROI was significantly larger than the NSD of the background region (Fig. 4 and 5).

The variations in NSD for the oversampling method, for sheets up to 0.5 mm thick, were noticeable because CT images of thinner sheets are more sensitive to noise. For the periodic QA, the long-term consistency of the measured values is necessary for providing alerts to even small changes in a machine, making the usage of thicker sheets advantageous. However, the correction factor increases rapidly with sheet thickness, as shown in Fig. 2; if this factor becomes too high, the noise in the MTF is also amplified by the factor from the equation (5), especially at high frequency. This is shown in Fig. 7(b) and (c) as the MTF 10 and MTF 5 from the 1.0 mm and 1.2 mm sheets have significant variation, while showing negligible variation in Fig. 7(a) for MTF 50. These inaccuracies are reflected in Fig. 6 where the 1.0 mm and 1.2 mm sheets have a relatively large NSD (compared to other thicknesses). In this study, the maximum recommended thickness for LSF acquisition is 0.8 mm, wherein the correction factor does not exceed 2 at the cut-off frequency.

In most cases, the oversampling method had better results than the non-oversampling method from 6(a) and 6(b). A limited number of data points were used to derive the LSF and the MTF for the non-oversampling method, despite the use of thick sheets, so the gaps between these points were smoothed by linear interpolations. In other words, the limited data of the non-oversampling method means that the noise attribution for one point in the high-frequency region can distort the overall results. This causes the considerable differences between two methods in Fig. 6(a) and (b), although they both occasionally show similar trends and accuracy.

The number of slabs does not seem to significantly improve the LSF estimation for the oversampling method (Fig. 6(c) and (d)). However, MTF 10 and MTF 5 with 1.0 mm and 1.2 mm sheets were more accurate with two slabs for the non-oversampling method. Nevertheless, if the oversampling method is used to acquire the LSF, with an appropriate sheet thickness (0.8 mm or less for this study), the different levels of beam hardening due to the thickness of the background material will not have significant impact on MTF measurements.

In the oversampling method, MTF measurement was insensitive to small angular variations ($< 1^{o}$), as shown in table 1 and 2, which exceeded the maximum deviation between users. Although the variations in MTF from the measurement of the 0.4 mm thick aluminum sheet were considerably larger than those of the 0.6 mm thick sheet, the effects from angle variation were similarly small. Therefore, the oversampling method for MTF measurement is reliable and consistent among the different users and sheet thicknesses, provided that the angle is carefully chosen.

Conclusion

Acquiring LSFs of various aluminum sheet thicknesses for MTF measurement provides consistent results except for sheets with a correction factor greater than 2 at the cutoff frequency. Although the non-oversampling method had comparable results with the oversampling method, its data were judged unreliable because of the interpolations between data points. Both the subjective choice of angulations for the oversampling method and the beam-hardening effects by the background slab thickness would not affect the resultant MTF significantly. Therefore, MTF derived from the oversampling method with

applying the thickness correction may be feasible for use in the periodic quality assurance program for CT, or other modalities, with the benefit of improved precision.

References

1. **Boone JM**: Determination of the presampled MTF in computed tomography. Medical Physics. 28(3):356 (2001)
2. **Garayoa J, Castro P**: A study on image quality provided by a kilovoltage cone-beam computed tomography. J Appl Clin Med Phys.14(1):3888 (2013)
3. **Villafana T**: Modulation transfer function of a finite scanning microdensitometer slit. Medical Physics. 2(5):251 (1975)
4. **Gopal A, Samant SS**: Use of a line-pair resolution phantom for comprehensive quality assurance of electronic portal imaging devices based on fundamental imaging metrics. Medical Physics. 36(6):2006 (2009)
5. **Nickoloff EL**: A simplified approach for modulation transfer function determinations in computed tomography. Medical Physics. 12(4):437 (1985)
6. **Fujita H, Tsai DY, Itoh T, Morishita, J, Ueda K, Ohtsuka A**: A simple method for determining the modulation transfer function in digital radiography. IEEE Trans Med Imaging.11(1):34-39 (1992)
7. **Nakaya Y, Kawata Y, Niki N, Umetatni K, Ohmatsu H, Moriyama N**: A method for determining the modulation transfer function from thick microwire profiles measured with x-ray microcomputed tomography. Medical Physics. 39(7):4347-4364 (2012)
8. **Schwarzband G, Kiryati N**: The point spread function of spiral CT. Phys Med Biol. 50(22):5307-5322 (2005)
9. **Watanabe H, Honda E, Kurabayashi, T**: Modulation transfer function evaluation of cone beam computed tomography for dental use with the oversampling method. Dentomaxillofac Radiol. 39(1):28-32 (2010)
10. **Yoo BG, Kweon DC, Lee JS**: MTF Evaluation and Clinical Application according to the Characteristic Kernels in the Computed Tomography. Korean J Med Phy. 18(2):55-64 (2007)
11. **Miéville F, Beaumont S, Torfeh T, Gudinchet F, Verdun F. R.**: Computed tomography commissioning programmes:how to obtain a reliable MTF with an automatic approach?. Radiation Protection Dosimetry. 139(1-3):443-448 (2010)
12. **Villafana T**: Effect of finite exposure slits in determination of the line spread function and modulation transfer function. Acta Radiol Ther Phys Biol. 16(3):281-288 (1977)
13. **Ohkubo M, Wada S, Matsumoto T, Nishizawa K**: An effective method to verify line and point spread functions measured in computed tomography. Medical Physics. 33(8):2757 (2006)
14. **Marchand E. W.**: Derivation of the Point Spread Function from the Line Spread Function. Journal of the Optical Society of America. 54(7):915-919(1964)
15. **Kayugawa A, Ohkubo M, Wada S**: Accurate determination of CT point-spread-function with high precision. J Appl Clin Med Phys. 14(4) (2013)
16. **Hyer DE, Serago CF, Kim S, Li JG, Hintenlang DE**: An organ and effective dose study of XVI and OBI cone-beam CT systems. J Appl Clin Med Phys. 11(2) (2010)
17. **Yagi M, Ueguchi T, Koizumi M, et al**: Gemstone spectral imaging:determination of CT to ED conversion curves for radiotherapy treatment planning. J Appl Clin Med Phys 14(5):173-186 (2013)

다양한 두께의 알루미늄 판을 이용한 MTF 측정에 관한 연구

동남권원자력의학원 *연구센터, †방사선종양학과

이동주*・김미영*・문영민†・정동혁*

본 연구에서는 방사선치료기용 CBCT의 영상과 같이 해상도가 낮은 경우에 적용할 수 있는 MTF (modulation transfer function) 평가 방법을 고안하였다. 본 연구에서는 두꺼운 알루미늄 판의 영상을 이용하여 중복 표본(oversampling) 방법과 두께 보정 방법을 적용하여 MTF를 결정하였다. 다양한 알루미늄 판의 두께(0.3~1.2 mm)에 대해 MTF를 분석하였으며 경사 영상과 평행 영상의 경우에 대해서도 비교하였다. 연구 결과 치료계획용 CT인 경우에 알루미늄의 두께가 0.8 mm 이하 일 경우 MTF 측정이 가능한 것으로 나타났다. 따라서 두꺼운 알루미늄 판과 두께 보정을 이용한 MTF 측정이 CT 영상에서 가능하였다.

중심단어: MTF, 영상공간분해능, 중복표본방법